GEOLOGY | THE GEOLOGICAL SOCIETY OF AMERICA®

https://doi.org/10.1130/G47089.1

Manuscript received 9 October 2019
Revised manuscript received 24 December 2019
Manuscript accepted 23 January 2020

Published online 18 March 2020

Experimental quantification of bedrock abrasion under oscillatory flow

James F. Bramante[1,2], J. Taylor Perron[2], Andrew D. Ashton[1] and Jeffrey P. Donnelly[1]
[1]Department of Geology & Geophysics, Woods Hole Oceanographic Institution, Woods Hole, Massachusetts 02543, USA
[2]Department of Earth, Atmospheric & Planetary Sciences, Massachusetts Institute of Technology, Cambridge, Massachusetts 02139, USA

ABSTRACT

Although wave-driven abrasion of submarine bedrock affects the evolution of rocky coasts and reefs globally, the dependence of the abrasion rate on wave forcing and sediment availability remains poorly quantified. We performed experiments in which an artificial substrate was abraded by varying amounts of coarse-grained sediment subjected to oscillatory flows. In these experiments, the bedrock incision rate scaled by the square of bedrock tensile strength (I, m yr^{-1} MPa^2) varied with mean root-mean-square (rms) velocity ($\langle u_{rms} \rangle$, m s^{-1}) according to a power law, $I = 1.0\langle u_{rms} \rangle^{4.2}$ (angle brackets indicate time-averaging over an entire experiment). Additionally, the relationship between sediment load and bedrock incision rate demonstrates tools and cover effects similar to abrasion in fluvial environments, such that incision is fastest at intermediate sediment loads. However, because oscillatory flows accumulate sediment into bedforms, the increased bedrock exposure reduces the efficiency of the cover effect for high sediment loads relative to unidirectional flow. Our results provide an empirical model that can be used to predict bedrock incision rates in nearshore environments based on wave forcing.

INTRODUCTION

In many coastal environments, waves drive loose sediment over exposed bedrock, eroding the bed and driving geomorphological change. On rocky shores, wave-driven abrasion can contribute to the downwearing of shore platforms (Blanco-Chao et al., 2007; Trenhaile, 2000). On coral reefs, wave-driven abrasion of the reef surface reduces net accretion rates and can produce spatially variable accretion (e.g., Grossman and Fletcher, 2004). Additionally, field observations (e.g., Cloud, 1954) and geostatistical analysis (Duce et al., 2016) suggest wave-driven abrasion drives the formation of fore-reef grooves. Understanding the evolution of hard-bottom coastal environments requires knowledge of the relationships between abrasion rate and wave and sediment characteristics.

Despite the prevalence of wave-driven abrasion on reefs globally, and its potential importance for rocky shores, few studies have measured the dependence of erosion on wave characteristics and sediment availability. On rocky shore platforms at the base of cliffs, vertical erosion by abrasion of up to 0.02 m yr^{-1} has been measured (Robinson, 1977; Blanco-Chao et al., 2007). Robinson (1977) observed that abrasion of the bedrock platform under beaches decreases with thickness of the overlying sediment, but that study had insufficient data to quantify the effect.

Abrasion by unidirectional flow in terrestrial bedrock channels is analogously important to the evolution of river landscapes. Laboratory experiments have constrained rate laws governing riverbed abrasion as a function of sediment flux and bedrock tensile strength. Rotary abrasion mill experiments (Sklar and Dietrich, 2001; Scheingross et al., 2014) demonstrated the existence of the tools and cover effects hypothesized by Gilbert (1877): Sediment impacts on the bed enhance abrasion, but as sediment load increases, sediment covers the bed, reducing the abrasion rate (Sklar and Dietrich, 2004). From these results, models have been developed to predict bedrock incision as a function of channel geometry, bedrock strength, and sediment characteristics (Sklar and Dietrich, 2006; Turowski et al., 2007; Lamb et al., 2008).

The unsteadiness of flow and sediment motion under waves may cause rate laws for wave-driven abrasion to deviate from those derived for steady flow in rivers. Theoretical and numerical models suggest that, in steady flows, the abrasion rate is determined by shear stress and sediment characteristics (Sklar and Dietrich, 2004; Lamb et al., 2008; Aubert et al., 2016). In contrast, under oscillatory flows, shear stresses and bed load flux vary over seconds-long time scales, the boundary layer is not fully developed, and normal stresses due to fluid acceleration can contribute to sediment transport (Fredsoe and Deigaard, 1992; Drake and Calantoni, 2001). Also, bedforms develop under oscillatory flow even when sediment sparsely covers the bed (e.g., Pedocchi and Garcia, 2009).

Here, we present results from experiments in which we used an oscillatory flow tunnel to quantify the abrasion rate of bedrock as a function of oscillation velocity and sediment load. We found that abrasion increases exponentially with oscillation velocity and exhibits tools and cover effects different from those observed in unidirectional abrasion mill experiments.

OSCILLATORY ABRASION EXPERIMENTS

To simulate wave-driven abrasion of submarine bedrock, we constructed a prototype oscillating u-tube (POUT) that consisted of a 2.45-m-long horizontal duct with rectangular cross section and two vertical reservoir pipes (Fig. 1A; Fig. DR1 in the GSA Data Repository[1]). Two thrusters and a control system generated and

[1]GSA Data Repository item 2020154, Figures DR1–DR4, Videos DR1–DR5 of bed forms, and Tables DR1 and DR2 (summarizing the videos and all experiments), is available online at http://www.geosociety.org/datarepository/2020/, or on request from editing@geosociety.org.

CITATION: Bramante, J.F., Perron, J.T., Ashton, A.D., and Donnelly, J.P., 2020, Experimental quantification of bedrock abrasion under oscillatory flow: Geology, v. 48, p. 541–545, https://doi.org/10.1130/G47089.1

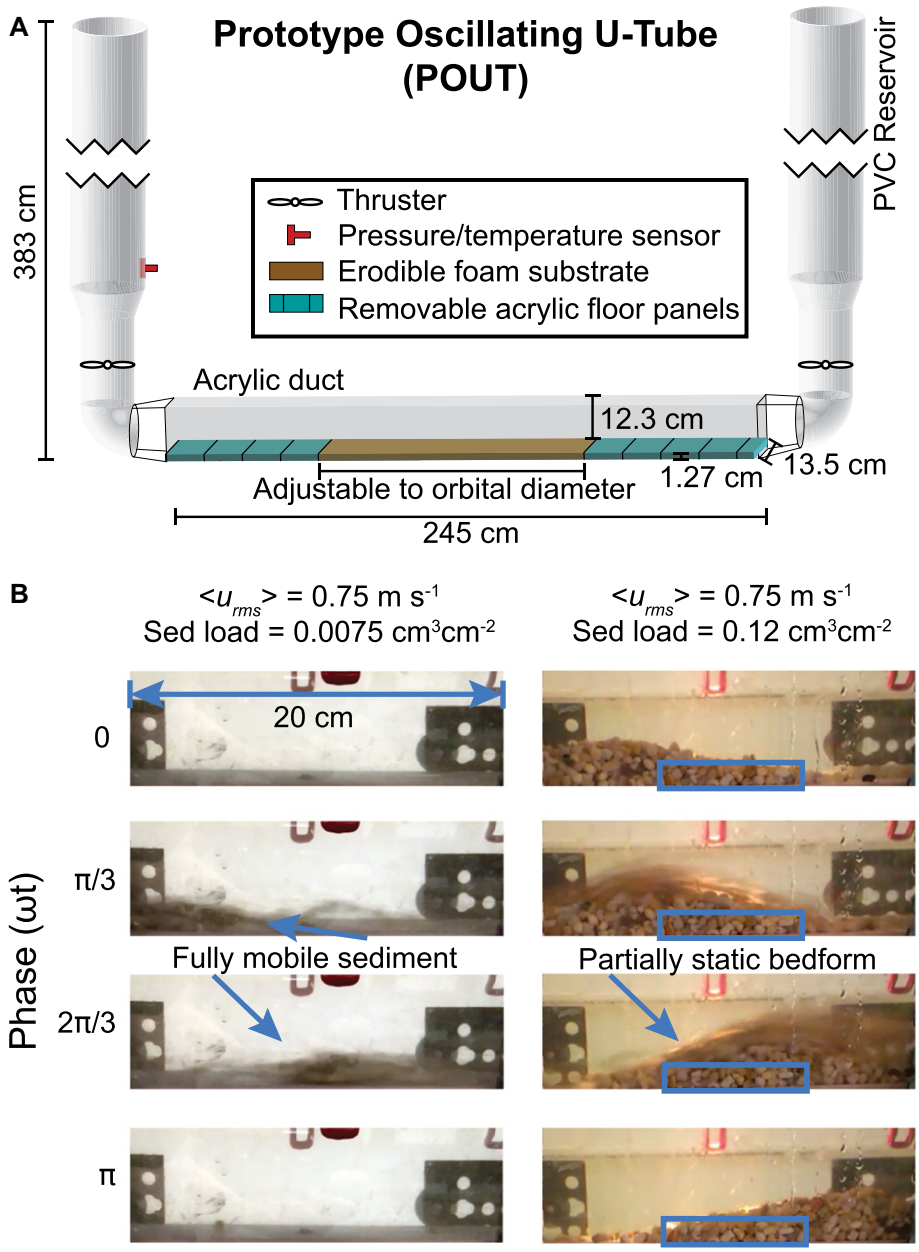

Figure 1. Experimental design and influence of bedforms. (A) Schematic drawing of the oscillatory flow tunnel. PVC—polyvinyl chloride. (B) Video stills from two experiments illustrating a fully mobile sediment band (left column) and a partially static isolated ripple (right column). Blue boxes indicate two layers of sediment grains that remain stationary during the entire wave period and cover the bed. Sediment had median (95% confidence interval) sieve diameter of D_{50} = 6.1 (4.2–7.6) mm and density ρ_s = 2570 (2300–2840) kg m^{-3}; $\langle u_{rms} \rangle$ is mean oscillation velocity time-averaged over an entire experiment.

maintained sinusoidal water-level fluctuations in the vertical reservoirs. When the POUT was filled, the water in the horizontal duct oscillated with a natural period of $T_s \approx 4.75$ s and with root-mean-square (rms) velocity (u_{rms}, m s^{-1}) of up to 1 m s^{-1}. Given a particular u_{rms} and T_s, the distance a water parcel travels during half of an oscillation is the orbital diameter, $d_o = \sqrt{2} u_{rms} T_s / \pi$.

To generate detectable erosion during short experiments, we used closed-cell urethane foam with low tensile strength (σ_T = 0.34–0.71 MPa), which varied between experiments due to differences between foam batches from the manufacturer, to simulate reef or bedrock substrate (Scheingross et al., 2014). The erosion rate was measured by weighing the foam and was normalized by the foam surface area and density to produce the incision rate. Because bedrock subjected to the low-velocity impacts of rolling or saltating sediment fails in tension (Sklar and Dietrich, 2001), and following previous experiments investigating the volumetric erosion rate of rock, concrete, and foam, we multiplied the incision rate by the square of the substrate tensile strength (σ_T^2; Sklar and Dietrich, 2001; Scheingross et al., 2014). (In situations where sediment instead slides on top of exposed bedrock, shear strength may be a more appropriate quantity for scaling abrasion rates.) The abrasion medium, subrounded siliciclastic gravel with sieve diameter D_{50} = 6.1 mm, was scattered uniformly across the duct floor and foam before initiation of each experiment. We refer to the average volume of gravel per unit area of the duct floor as sediment load, S (cm^3 cm^{-2}).

Upon initiation of oscillatory flow in each experiment, most of the sediment rapidly self-organized into one or more bedforms, leaving most of the duct floor covered only by scattered sediment grains. The morphology of the bedforms varied with S. At low S (0.0075–0.015 cm^3 cm^{-2}), the bedforms consisted of mobile bands 1–2 grain diameters thick and 10–30 grain diameters wide that migrated over distances much greater than their width (Fig. 1B; Videos DR1 and DR2). In experiments with high S (≥0.12 cm^3 cm^{-2}), the bedforms consisted of mounds several grain diameters high with appearance similar to rolling-grain ripples (Fig. 1B; Videos DR3 and DR4; Pedocchi and Garcia, 2009). Motion of these mounds differed between low (<0.75 m s^{-1}) and high (≥0.75 m s^{-1}) u_{rms}. In low-u_{rms}/moderate-S and high-u_{rms}/high-S experiments, the mounds had a stationary core, and sediment saltated from the stoss face of a mound, over the mound crest, to the bare substrate on the lee side every half-oscillation (Fig. 1B; Videos DR3 and DR4). In high-u_{rms}/moderate-S experiments, the mounds migrated back and forth in their entirety, primarily through saltation (Fig. 1B; Video DR5).

The isolated bedforms in our experiments with high-S resembled isolated ripples of sand-sized sediment observed in the field. For example, on the Ningaloo Australia fringing reef, large wave events expose bare substrate that is covered by coarse sand ripples (Rosenberger et al., 2019). On mixed sand-gravel beaches, isolated ripples form on otherwise immobile beds when flows are insufficiently strong to mobilize gravel (Hay et al., 2014).

The number and spacing of bedforms in our experiments tended to increase with increasing S and decrease with increasing u_{rms} (Fig. DR2). When two to three bedforms formed, their spacing scaled with d_o (range: 0.6d_o–1d_o) and was consistent with field observations of orbital ripple spacing in coarse sediment beds (Fig. DR3; Pedocchi and Garcia, 2009). Because these bedforms produced spatial variability in the abrasion rate, the foam was cut to the length of one full bed-form spacing (0.8d_o). Because only one bedform would be located on the foam, we normalized S in each experiment by the number of bedforms, which we will refer to as normalized sediment load (S*, cm^3 cm^{-2}).

We performed two sets of experiments using the POUT (Table DR2). In the first set,

we held S constant at either 0.03 cm^3 cm^{-2} or 0.12 cm^3 cm^{-2} and varied u_{rms} in the range 0.4–1.0 m s^{-1}. In the second set, we held u_{rms} constant at 0.5, 0.6, or 0.75 m s^{-1} and varied S over 0.0075–0.48 cm^3 cm^{-2}.

CONTROLS ON BEDROCK INCISION

Across all experiments, mean incision rate of the bedrock simulant increased with u_{rms} (Fig. 2), which is described well by a power law of the form:

$$I = C_t K \langle u_{rms} \rangle^n, \quad (1)$$

where I is incision rate scaled by σ_T^2 (m yr^{-1} MPa^2); $C_t = 3.15 \times 10^7$ s yr^{-1} is a conversion factor for time; K is a constant [$s^{(n-1)}\, m^{-(n-1)}$ MPa^2]; angle brackets ($\langle\rangle$) indicate time-averaging over an entire experiment; and n is a dimensionless exponent. A nonlinear least-squares fit provided estimates (95% confidence interval) of $n = 4.2$ (3.6, 4.8) and $C_tK = 1.0$ (0.7, 1.3), with $R^2 = 0.86$. Thus, incision rate scales with u_{rms} raised to a power of ~4.

For a given u_{rms}, the relationship between the incision rate and S was characterized by tools and cover effects (Fig. 3), where the incision rate increased with increasing S* until reaching a maximum (tools effect) and then decreased with increasing S* (cover effect). The shape of our inferred tools and cover effect was similar to that found in rotary mill experiments (Sklar and Dietrich, 2001), but it had a slower decay of incision rate, indicating a weaker cover effect. The tools and cover effects can be modeled with a power function of sediment mass (T17; Turowski and Hodge, 2017). Applied to the abrasion mill experiments, T17 collapses to a special case in which additional sediment falls equally on exposed and already covered bedrock (Turowski et al., 2007). In our experiments, however, the best fit of T17 indicates that sediment is preferentially sequestered in bedforms, reducing the cover effect (Fig. 3).

The transition from the tools effect to the cover effect can be observed in the spatial pattern of abrasion. For low S, the incision rate reached a maximum at the center of the range of bedform motion (Fig. 4A), because the entire bedform was mobilized during each flow oscillation. However, for high S, a portion of the bedform remained immobile, and incision rates were lowest under the center of the bedform and highest at the bed-form edges, where sediment saltated vigorously (Fig. 4A). For a constant, high S, a large portion of the bed under the bedform was covered at low u_{rms}, whereas the same region experienced maximum incision rates at higher u_{rms} as the bedform was fully mobile (Fig. 4B).

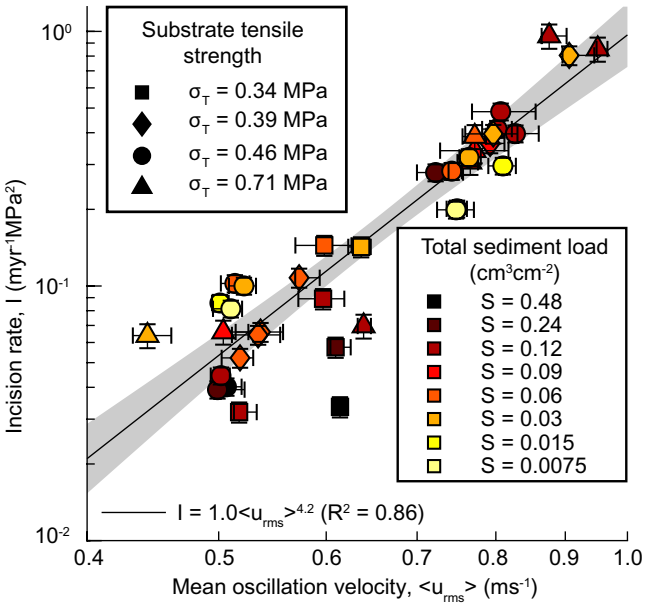

Figure 2. Relationship between mean oscillation velocity and bedrock incision rate. Black line is the nonlinear least-squares fit of power law to all data. Gray shading indicates 95% confidence interval of fit. Vertical error bars represent ±1 standard deviation in mean incision rate as estimated from Monte Carlo uncertainty analysis in which measurement uncertainty and variability in material properties (foam weight, foam density, and foam tensile strength) were propagated through the incision rate calculation 10,000 times for each experiment. Horizontal bars indicate interquartile range of oscillation velocity during each experiment. Incision rate was calculated as $I = (m_{pre} - m_{post})/(A_{sub} \times \rho_{sub} \times t_{exp})$, where m_{post} is post-experimental weight after foam was dried in an oven at 100 °C for 8 h, m_{pre} is pre-experiment weight, t_{exp} is experiment duration, A_{sub} is the foam's exposed surface area, and ρ_{sub} is foam density.

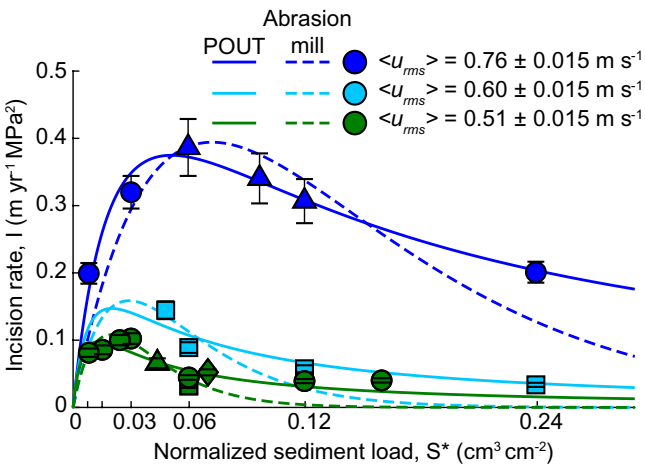

Figure 3. Influence of sediment availability on bedrock incision rate. Vertical error bars represent ±1 standard deviation of the mean incision rate as estimated in Monte Carlo uncertainty analysis. Symbol definitions are as in Figure 2; $\langle u_{rms} \rangle$ is mean oscillation velocity time-averaged over an entire experiment. Lines are nonlinear least squares fits of $I = k_1 S^*[1 - (1 - k_2)k_3 S^*]^{\wedge}[1/(1-k_2)]$ (T17; Turowski and Hodge, 2017, their equation 9) to data in the figure, where k_1 is free parameter accounting for sediment characteristics; k_2 modulates the probability (P) that additional sediment falls on exposed or covered bedrock; and k_3 accounts for maximum instantaneous bed-load flux at a given velocity. Single values of k_1 and k_2 were optimized for all data in the figure, while k_3 was allowed to vary for each of three orbital velocities. For the dashed line, k_2 was set constant at 0.999, equivalent to abrasion mill case (Turowski et al., 2007). For the solid line, $k_2 = 1.46$ was optimized from all data. POUT—prototype oscillating u-tube.

DISCUSSION

Sediment Controls on Wave-Driven Abrasion and Reef Morphology

Our experiments demonstrate that the abrasion rate under oscillatory flow increases exponentially with orbital velocity and that S provides a secondary control through tools and cover effects. The transition of bedforms from fully mobile to partially static appears to mark the transition in dominance from the tools to the cover effect. The power-law dependence of abrasion rate on oscillation velocity implies a strong feedback between water depth and abrasion rate, because the orbital velocity under waves decreases rapidly with increasing depth (Fig. DR4). Thus, as a surface lowers through wave-driven abrasion, the abrasion rate will decrease rapidly, a negative feedback relationship that likely influences the temporal evolution and equilibrium state of landforms such as shore platforms and fore-reef grooves.

The magnitude of the incision rates observed in our experiments also demonstrates the potential importance of abrasion for the evolution of nearshore environments. For example, the tensile strength of reef-building corals is typically 1.0–3.2 MPa, while the reef substrate on which the corals grow has lower tensile strength, typically 0.2–0.8 MPa (Madin, 2005; Madin et al., 2013). Typical trade wind–driven waves in the central North Pacific ($H_s = 1.5$ m, $T_p = 8$ s;

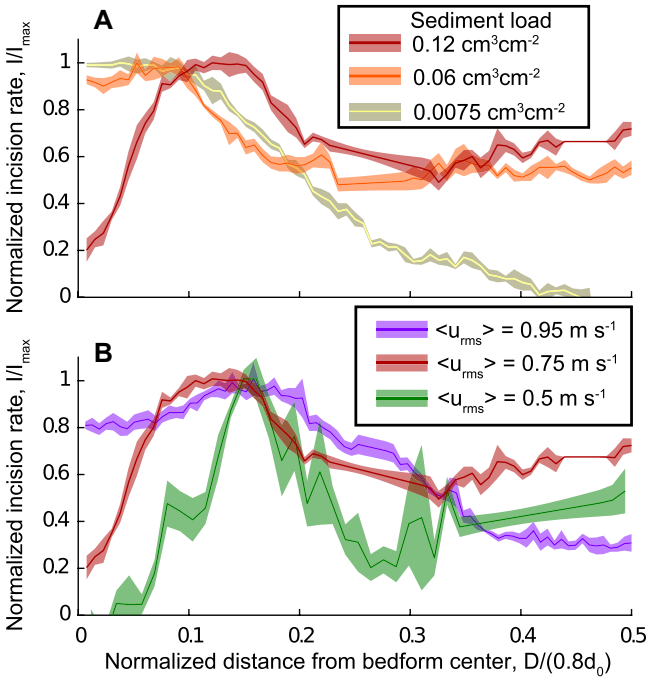

Figure 4. Variability in abrasion rate with position relative to bedforms. Incision rate was measured along the length of foam substrate demonstrating the influence of bedforms in three experiments: (A) with mean oscillation velocity time-averaged over an entire experiment $\langle u_{rms} \rangle = 0.75$ m s^{-1}, including those in Figure 1B, and (B) with sediment load $S^* = 0.12$ cm^3 cm^{-2}. Incision rates were normalized by the maximum incision rate in each profile. Lines (shading) indicate mean (±1 standard deviation) of the four replicate outside micrometer measurements made at 1 cm intervals down the length of the foam substrate.

Shope et al., 2016) generate $u_{rms} = 0.76$ m s^{-1} in water 4 m deep. If sediment availability were within the range of our experiments, these waves would produce incision rates of 0.3–10 m yr^{-1} for reef substrate and 0.02–0.4 m yr^{-1} for coral. In contrast, the maximum measured rates of reef accretion and individual coral growth are ~0.02 m yr^{-1} and ~0.2 m yr^{-1}, respectively (Montaggioni, 2005). However, care should be taken when applying our results to field settings because abrasive tools erode themselves, with associated impacts against bedrock and other tools, especially if the tools have similar tensile strength as the bedrock.

Assuming that abrasive tools are rapidly replaced on productive reefs, the incision rates implied by our experiments would overwhelm reef accretion and coral growth. The fact that net reef accretion occurs at all implies that sediment capable of generating appreciable abrasion is scarce on reef surfaces, particularly as sediment cover would also hinder coral growth. However, shore-normal grooves common to fore reefs often contain a thin veneer of coarse sediment and show signs of abrasion (Duce et al., 2016; Cloud, 1954). Grooves, which potentially form through abrasion, may promote reef growth by sequestering abrasive tools from the reef surface. Here, we have also quantified the tools and cover effects under oscillatory flow, providing a framework to better study the complex feedbacks among reef accretion, sediment production, and sediment transport that likely give rise to spur and groove features on fore reefs.

Comparison to Fluvial Bedrock Abrasion

The dependence of abrasion rate on orbital velocity in our experiments is similar to that found for abrasion under unidirectional flow. Numerical modeling of bedrock abrasion under unidirectional flow suggests that the abrasion rate exhibits a power-law dependence on excess shear stress, with the exponent ranging from 1 to 3 depending on sediment load (Aubert et al., 2016). Sediment in that numerical model had a negligible threshold of motion, so assuming that excess shear stress varies roughly with shear stress, which scales with velocity squared (Fredsoe and Deigaard, 1992), the abrasion rate in the numerical model varied with flow velocity raised to a power of 2–6, bracketing our estimate for oscillatory flow. Additionally, the power-law exponent increased with increasing sediment load, which is consistent with our results (Fig. 2). However, the cover effect in our experiments was weaker than in the abrasion mill experiments for unidirectional flow. Theoretically, the cover effect in bedrock rivers can differ from the abrasion mill experiments, but here we demonstrate a causal link between bedform formation and a reduced cover effect. The decrease in abrasion rate with distance from the edge of the bedforms implies that there is also spatial variability in the tools effect, which has been assumed absent in fluvial abrasion.

CONCLUSIONS

Wave-driven abrasion has long been hypothesized to be an important driver of coastal change, but its dependence on wave characteristics and sediment availability has been poorly quantified. Our experiments demonstrate that abrasion rates increase as a power function of wave orbital velocity and exhibit tools and cover effects with sediment load that are distinct from fluvial abrasion. We provide an empirical relationship between oscillation velocity and incision rate that predicts coastal bedrock abrasion rates from typical wave characteristics.

ACKNOWLEDGMENTS

We thank the Massachusetts Institute of Technology (MIT) Makerworkshop for material assistance. This study was supported by the U.S. Department of Defense Strategic Environmental Research and Development Program through award SERDP RC-2336, by the Woods Hole Oceanographic Institution Ocean Venture Fund, and by the MIT Department of Earth, Atmospheric and Planetary Sciences Student Research Fund. We also thank Jens Turowski and an anonymous reviewer for their insightful comments on our manuscript.

REFERENCES CITED

Aubert, G., Langlois, V.J., and Allemand, P., 2016, Bedrock incision by bedload: Insights from direct numerical simulations: Earth Surface Dynamics, v. 4, p. 327–342, https://doi.org/10.5194/esurf-4-327-2016.

Blanco-Chao, R., Perez-Alberti, A., Trenhaile, A.S., Coosta-Casais, M., and Valcarcel-Diaz, M., 2007, Shore platform abrasion in a para-periglacial environment, Galicia, northwestern Spain: Geomorphology, v. 83, p. 136–151, https://doi.org/10.1016/j.geomorph.2006.06.028.

Cloud, P.E., Jr., 1954, Superficial aspects of modern organic reefs: The Scientific Monthly, v. 79, p. 195–208.

Drake, T.G., and Calantoni, J., 2001, Discrete particle model for sheet flow sediment transport in the nearshore: Journal of Geophysical Research, v. 106, p. 19859–19868, https://doi.org/10.1029/2000JC000611.

Duce, S., Vila-Concejo, A., Hamylton, S.M., Webster, J.M., Bruce, E., and Beaman, R.J., 2016, A morphometric assessment and classification of coral reef spur and groove morphology: Geomorphology, v. 265, p. 68–83, https://doi.org/10.1016/j.geomorph.2016.04.018.

Fredsoe, J., and Deigaard, R., 1992, Mechanics of Coastal Sediment Transport: Singapore, World Scientific Publishing Co. Pte. Ltd., 369 p., https://doi.org/10.1142/1546.

Gilbert, G.K., 1877, Report on the Geology of the Henry Mountains: Geographical and Geological Survey of the Rocky Mountain Region: Washington, D.C., Government Printing Office, 106 p., https://doi.org/10.3133/70039916.

Grossman, E.E., and Fletcher, C.H., III, 2004, Holocene reef development where wave energy reduces accommodation space, Kailua Bay, Windward Oahu, Hawaii, U.S.A.: Journal of Sedimentary Research, v. 74, p. 49–63, https://doi.org/10.1306/070203740049.

Hay, A.E., Zedel, L., and Stark, N., 2014, Sediment dynamics on a steep, megatidal, mixed, sand-gravel-cobble beach: Earth Surface Dynamics, v. 2, p. 443–453, https://doi.org/10.5194/esurf-2-443-2014.

Lamb, M.P., Dietrich, W.E., and Sklar, L.S., 2008, A model for fluvial bedrock incision by impacting suspended and bed load sediment: Journal of Geophysical Research, v. 113, F03025, https://doi.org/10.1029/2007JF000915.

Madin, J.S., 2005, Mechanical limitations of reef corals during hydrodynamic disturbances: Coral Reefs, v. 24, p. 630–635, https://doi.org/10.1007/s00338-005-0042-0.

Madin, J.S., Dell, A.I., Madin, E.M.P., and Nash, M.C., 2013, Spatial variation in mechanical properties of coral reef substrate and implications for

coral colony integrity: Coral Reefs, v. 32, p. 173–179, https://doi.org/10.1007/s00338-012-0958-0.
Montaggioni, L.F., 2005, History of Indo-Pacific coral reef systems since the last glaciation: Development patterns and controlling factors: Earth-Science Reviews, v. 71, p. 1–75, https://doi.org/10.1016/j.earscirev.2005.01.002.
Pedocchi, F. and Garcia, M.H., 2009, Ripple morphology under oscillatory flow: 1. Prediction: Journal of Geophysical Research, v. 114, C12014, https://doi.org/10.1029/2009JC005354.
Robinson, L.A., 1977, Erosive processes on the shore platform of northeast Yorkshire, England: Marine Geology, v. 23, p. 339–361, https://doi.org/10.1016/0025-3227(77)90038-X.
Rosenberger, K., Storlazzi, C., Pomeroy, A., Cheriton, O., Lowe, R., and Hansen, J., 2019, Spatial and temporal variability in ripple formation and migration across a coral reef flat and lagoon, *in* Wang, P., et al., eds.,Proceedings of the 9th International Conference on Coastal Sediments: Singapore, World Scientific, p. 983–990.
Scheingross, J.S., Brun, F., Lo, D.Y., Omerdin, K., and Lamb, M.P., 2014, Experimental evidence for fluvial bedrock incision by suspended and bedload sediment: Geology, v. 42, p. 523–526, https://doi.org/10.1130/G35432.1.
Shope, J.B., Storlazzi, C.D., Erikson, L.H., and Hegermiller, C.E., 2016, Changes to extreme wave climates of islands within the Western Tropical Pacific throughout the 21st century under RCP 4.5 and RCP 8.5, with implications for island vulnerability and sustainability: Global and Planetary Change, v. 141, p. 25–38, https://doi.org/10.1016/j.gloplacha.2016.03.009.
Sklar, L.S., and Dietrich, W.E., 2001, Sediment and rock strength controls on river incision into bedrock: Geology, v. 29, p. 1087–1090, https://doi.org/10.1130/0091-7613(2001)029<1087:SARSCO>2.0.CO;2.
Sklar, L.S., and Dietrich, W.E., 2004, A mechanistic model for river incision into bedrock by saltating bed load: Water Resources Research, v. 40, W06031, https://doi.org/10.1029/2003WR002496.
Sklar, L.S., and Dietrich, W.E., 2006, The role of sediment in controlling steady-state bedrock channel slope: Implications of the saltation-abrasion incision model: Geomorphology, v. 82, p. 58–83, https://doi.org/10.1016/j.geomorph.2005.08.019.
Trenhaile, A.S., 2000, Modeling the development of wave-cut shore platforms: Marine Geology, v. 166, p. 163–178, https://doi.org/10.1016/S0025-3227(00)00013-X.
Turowski, J.M., and Hodge, R., 2017, A probabilistic framework for the cover effect in bedrock erosion: Earth Surface Dynamics, v. 5, p. 311–330, https://doi.org/10.5194/esurf-5-311-2017.
Turowski, J.M., Lague, D., and Hovius, N., 2007, Cover effect in bedrock abrasion: A new derivation and its implications for the modeling of bedrock channel morphology: Journal of Geophysical Research, v. 112, F04006, https://doi.org/10.1029/2006JF000697.

Printed in USA